NEURONAL ACTIVITY IN OLFACTORY PROCESSING: A META-ANALYSIS AND EXPERIMENTAL STUDY

Ethan Abramovitz, Grace Calhoun, Emily Chen, Maanav Chittireddy, Sapna Patel, Survani Sinha, Titus Solomon, Joshitha Sripada, Arjun Subramanian, Hillary Xie, Jessica Yao

Advisor: Graham Cousens, Ph.D.
Assistant: Harris Naqvi, B.S.

ABSTRACT

When the brain processes odorant molecules, olfactory receptor neurons (ORNs) in the olfactory epithelia project cilia into the nasal mucosa, providing our sense of smell. However, research shows that when ORNs process odorants, inhibition occurs. To address this phenomenon, we wanted to find: 1) differences in inhibition/excitation between brain regions, 2) how inhibition varies for different functional groups, and 3) if inhibition occurs simultaneously between neurons in oscillatory patterns. By examining mouse olfactory systems through single-unit electrophysiological recordings from our lab and other studies, we generated plots using MATLAB to analyze the firing rates of odor-cell pairs when exposed to different scents. We hypothesize that odor-invoked neuronal responses in the olfactory bulb will show a higher proportion of excitatory responses than primary cortical regions; simultaneous responses will be detectable between neurons of the same cortical region; neurons will show oscillatory spiking patterns with dominant frequency components in the beta and gamma bands; and the degree of mixture suppression would directly correlate to the similarity between functional groups. Through our meta-analysis and experiment, we found that inhibition was most prevalent in early olfactory regions such as the olfactory bulb (OB) and piriform cortex (PC), but substantially lower in higher-order areas like the posterolateral cortical amygdala (plCoA) and dorsal tenia tecta (TT). This supports a hierarchical model in which inhibition has a key role in odor filtering but has a lesser role in downstream regions involving higher-order functions.

INTRODUCTION

Despite being essential for emotional regulation and survival in many species, the olfactory system remains one of the least researched sensory systems. To expand research in this field, we examined olfactory information processing in components of the mouse brain's olfactory system using extracellular single-unit recordings. We conducted a meta-analysis of secondary data and corroborated our findings with the results of our experiment. Specifically, our team focused on various forms of inhibition in various olfactory regions. We explored our goals using two methods: first, an analysis of single-unit electrophysiological data from three previously published studies, and second, a novel experiment that explored mixture suppression, with a focus on the anterior olfactory nucleus (AON). The objective of the latter experiment was to explore potential variation in the degree of mixture suppression within the AON between different chemical classes using mixtures of esters and terpenes.

Anatomy

The olfactory system begins with the detection of odorants and progresses into complex regions, each responsible for organization, identification, or processing. Within the olfactory epithelium exist the olfactory receptor neurons (ORNs) (1). ORNs project cilia into the nasal mucosa, which contains olfactory receptors (ORs), thereby increasing the surface area available for odorants to bind (2). Each ORN expresses only one type of receptor, allowing odors to be traced spatially; namely, ORNs map to two glomeruli, one on the lateral side and one on the medial side of the olfactory bulb (3). Each glomerulus receives projections from only one type of ORN, and different odors activate a unique combination of glomeruli, which form distinct spatial clusters in the olfactory bulb. Mice have roughly 1000 distinct ORs, each of which is selectively responsive to an odorant's functional groups and molecular profile, such as carbon chain length or structure. However, this means that odorants with similar functional groups could trigger the same type of receptor (4).

After odorant binding initiates, the axons of the ORNs move through the cribriform plate and bind to glomeruli within the main olfactory bulb (OB). There are clusters of glomeruli that integrate distinct functional groups. For example, aldehydes, which are generally perceived as oily, are mapped to the dorsal-anterior region of the olfactory bulb; esters, which are perceived as fruity, are mapped to a similar cluster; and terpenes, which are perceived as citrusy or woody, are mapped to the medial region of the olfactory bulb (4). These glomeruli help to segregate olfactory processing and primarily serve to project to the dendrites of second-order neurons, specifically the mitral and tufted cells (5). Mitral cells receive information from cells in a single glomerulus with their primary dendrite, while also receiving information from additional signals from inhibitory interneurons, such as the granule cells. These neurons project to the entire olfactory cortex. Meanwhile, tufted cells perform the same function, but innervate a smaller part of the brain and reach only the AON and olfactory tubercle (6, 3).

Additionally, ORNs can exhibit broad tuning (activation by a wide range of different odorants) or narrow tuning (activation by typically only one odorant, thus expressing only one type of olfactory receptor protein) (7, 8). Broadly tuned ORNs can signal the presence of an ester, for example, instead of identifying a single odorant; narrowly tuned ORNs can identify specific odorants, even in the presence of complex mixtures (9). The outputs processed by the mitral and tufted cells are then transmitted primarily through the lateral olfactory tract (LOT), which courses along the ventrolateral surface of the olfactory peduncle and cerebrum in the mouse. The LOT is a tract composed of the axons of mitral and tufted cells that project to many primary olfactory areas, with the PC being the most prominent.

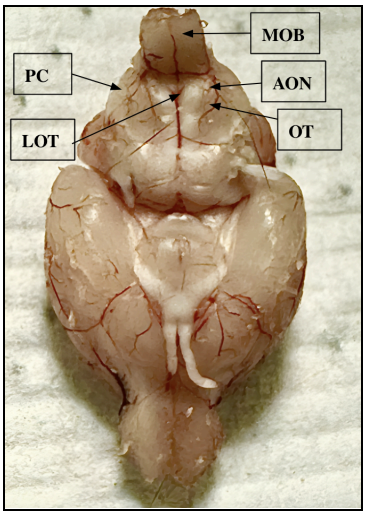

Figure 1. Diagram of a mouse brain displaying the main olfactory bulb (OB), piriform cortex (PC), anterior olfactory nucleus (AON), lateral olfactory tract (LOT), and olfactory tubercle (OT). Taken from a mouse we performed electrophysiological recordings on. Not shown are the lateral entorhinal cortex (LEC) and cortical nuclei of the amygdala, which also receive direct input from the OB.

The information the PC receives directly from the OB is distributed diffusely across the PC, differing from other primary olfactory areas that receive localized projections. Unlike other sensory cortices, the PC lacks spatial organization of the odors it receives. Instead, it uses population code, which groups the activity of clusters of neurons to discriminate between and integrate odor identities (10). The PC is typically divided into two subregions, the anterior and the posterior (11). The anterior focuses on encoding odor identity, while the posterior's function relates to odor categorization and associative memory (12). Important neurons in the PC include pyramidal cells, which receive input from mitral cells of different glomeruli, allowing for a combinatory encoding of different odor identities. Layer 1a of the PC receives its information from mitral and tufted cells through the LOT, where the LOT axons synapse onto the distal dendrites of pyramidal neurons.

The broader olfactory system encompasses numerous other primary olfactory regions involved in regulating emotions, memories, and movement, enabling a complex interpretation of olfactory input (13). These areas include the AON, TT, olfactory tubercle (OT), plCoA, and entorhinal cortex (EC), which all contribute to high-order processing such as memory formation and behavioral output (14). The AON belongs to a highly intertwined bilateral network that sends feedback projections directly to the OB and forward projections to the hypothalamus, PC, and TT (15). The TT receives information from the OB, PC, and EC and may serve as a bridge that links input from the primary cortical regions to the secondary limbic regions. Composed of the dorsal tenia tecta (DTT) and ventral tenia tecta (VTT), the tenia tecta is anatomically adjacent to the hippocampal formation and olfactory tubercle and plays an integral role in memory systems (16). The plCoA receives direct input from the OB and the cortical amygdala. This region plays a significant role in innate odor-driven behaviors by associating olfactory signals with emotional and survival circuits, such as predator avoidance and mating (10). Acting as a relay system from the olfactory bulb to the hippocampus, the entorhinal cortex allows for the

formation of long-term memories. More specifically, the lateral EC receives input from the PC and AON to relay information to the hippocampus, enabling the processing of odor-context associations and spatial memories (17). These higher-order structures form a distributed network that coordinates with the OB and PC to ensure that sensory information is effectively encoded and stored. Unlike the primary olfactory regions, higher-order areas exhibit neural activity patterns that influence associative feedback (16).

Inhibition

Excitatory pyramidal neurons act as the main integrators and output units of the limbic olfactory areas. These neurons work in tandem with inhibitory interneurons, which help modulate local and long-range circuit connections. Inhibition plays a crucial role in the olfactory cortex, with two primary types of inhibitory control: feedforward inhibition and feedback inhibition. Feedforward inhibition occurs when a principal neuron is connected to another neuron and an inhibitory interneuron. Activation of the principal neuron leads to the excitation of the target neuron as well as a local inhibitory interneuron. In turn, the interneuron inhibits the downstream neuron, limiting the neuron's excitatory response and also helping to refine the flow of information within the neural section (18). In contrast, feedback inhibition involves a reciprocal relationship between a principal neuron and an interneuron.

Upon activation, the principal neuron excites the interneuron, which then projects back to inhibit the primary principal neuron, forming a self-regulating loop that aids in preventing the overexcitation of the principal neuron. These pathways enable precise control of neural activity, resulting in more accurate and efficient signal processing (19).

Oscillations

Within the brain, neurons fire at different frequencies or oscillations. These frequencies have been given the name oscillations, as they are closely linked to the respiratory cycle and play a crucial role in odor learning and odor discrimination. The PC and OB may undergo coupling, which is characterized by the synchronization of rhythms between different brain regions. In the olfactory system, there are three unique types of oscillations: beta, theta, and gamma (20). Known as respiratory oscillations, theta oscillations are commonly found in the OB and PC and range in frequency from 1 to 12 Hz. These oscillations couple with hippocampal theta waves to support odor processing. Gamma oscillations are the fastest known oscillations, encompassing an extensive range of frequencies between 30-120 Hz that peak around 70 Hz in both mice and humans and are evoked through sensory stimulation. Mainly associated with high-level cognition, such as odor discrimination between structurally similar odorants, they originate from reciprocal excitatory–inhibitory interactions between mitral and granule cells (20).

In the PC, gamma oscillations are typically seen to couple with OB gamma oscillations (20). Typical ways to predict the amplitude of gamma oscillations, especially in the PC or OB, are through the spikes of pyramidal cells. There also exists a lower frequency variant of gamma oscillations, called gamma2, which ranges from 50 to 60 Hz. Beta oscillations typically occur in the frequency range of 15-30 Hz. In contrast to the other oscillations, beta oscillations can span

anywhere from 2 to 4 respiration cycles and are closely related to odor learning and behavioral relevance. Although the cellular origins of oscillations are still unclear, beta oscillations can be seen across the OB, PC, and hippocampus. This large span of regions suggests that beta rhythms rely on broader networks to integrate memory and sensory input.

Our Work

Given that no singular dataset provides a comprehensive picture of how inhibition varies across regions of the olfactory system, odorant types, and phases of the respiratory cycle, we employed a meta-analysis to examine some features of inhibition across several olfactory areas. Combining data and findings from various studies allows us to evaluate studies that explore similar topics but vary in their methods, scope, or focus. This meta-analytic approach enables us to aggregate data and create a robust dataset across multiple olfactory cortices, thereby forming a broader conclusion about olfactory research. In our project on olfactory processing in mice, we specifically chose this method to synthesize results across several experiments that investigate how different brain regions respond to various odors and examine the role of inhibition.

To understand the complex olfactory system, researchers use electrophysiology recording techniques to gather data on the electrical activity of neurons. One prominent technique is single-unit recording. It involves inserting a microelectrode into the brain of an anesthetized mouse to capture the electrical activity of individual neurons or small clusters of neurons. Single-unit recording offers highly accurate and sensitive measurements while maintaining cost-effectiveness, allowing researchers to obtain high-quality data (21, 22). The three primary studies used in our meta-analysis are Cousens (2020), Bolding & Franks (2018), and Iurilli & Datta (2017) (21, 32, 10). We analyzed and synthesized data from these studies, which explore various parts of the olfactory cortex (PC, OB, AON, TT, plCoA) to understand their functional roles and behavior, and signaling dynamics. For instance, Cousens (2020) conducted single-unit recordings in anesthetized mice to assess odor-evoked activity across olfactory regions while also observing respiration patterns (21). Bolding & Franks (2018) investigated the PC by blocking feedback inhibitory interneurons from releasing neurotransmitters to analyze the behavior of the PC about the OB (32). Iurilli & Datta (2017) found that, like the PC, plCoA uses distributed population coding to represent a multitude of signals with various combinations of neuron patterns (10). We explored excitation and inhibition in the OB and several target regions about: (a) Alterations in odor-elicited firing rates, including excitatory and inhibitory responses to chemicals of varying structures; (b) Rhythmicity of neural firing about the three primary oscillatory frequencies known to occur in olfactory structures, as revealed by autocorrelation; (c) Correlated activity between simultaneously recorded cell pairs as revealed by cross-correlation analysis.

Aside from meta-analysis, we also conducted experiments to explore the features of response inhibition in the AON. Response inhibition is a phenomenon reported in PC and other olfactory regions involving a reduction in excitatory response to mixtures of odorants, relative to single odorants, or sublinear summation of odor-elicited excitation. This allowed us to further investigate the role of functional groups in olfaction, extending beyond previously published works. There is evidence for mixture suppression in the PC, both for odorants with distinct and

similar functional groups. Up to 60% of neurons exhibited inhibition when exposed to a mixture of odorants, but not when those odorants were presented alone (23).

Hypotheses

Given our guiding research from the previous studies mentioned, we formulated 3 hypotheses. First, we hypothesized that odor-evoked neuronal responses in the OB will show a higher proportion of excitatory responses than primary cortical regions (PC, pLCoA, TT, AON). The olfactory bulb is the first central relay for olfactory information and directly receives input from ORNs. In contrast, the primary olfactory cortical regions integrate inputs from multiple OB outputs and are subject to more complex modulation, including inhibitory processing. Next, we hypothesized that simultaneous excitatory coupling between pairs of neurons would be detectable within the same cortical region and show oscillatory spiking patterns with dominant frequency components in the beta and gamma bands. Olfactory cortical areas, especially PC and AON, are known to exhibit oscillatory activity in the beta (15-35 Hz) and gamma (40-80 Hz) bands during odor processing. This synchronous firing is thought to support functions like odor discrimination, memory formation, and attention. Gamma oscillations, in particular, are associated with local circuit synchrony, while beta may reflect long-range coordination. Finally, we hypothesized that the degree of mixture suppression would be related to the degree of similarity between odorants; with similar classes of odorants (ex., terpene-terpene or ester-ester) resulting in the most suppression, and less suppression across classes (e.g., terpene-ester). When structurally similar odorants are presented together, they are more likely to activate overlapping populations of ORNs and glomeruli, which can lead to competitive or suppressive interactions. Similar odorants can saturate shared neural pathways, effectively masking each other. Conversely, chemically dissimilar odorants activate more distinct sets of ORNs, reducing the chance for mutual suppression.

METHODS

Secondary Data Analysis

Data Analysis

All analyses were conducted using custom scripts written in MATLAB. Spike waveforms were extracted and isolated from various datasets by following the studies conducted by Cousens (2020), Bolding & Franks (2018), and Iurilli & Datta (2017) (21, 32, 10). Cousens (2020) recorded odor-evoked activity in the DTT and VTT, both underrepresented in olfactory processing research, to compare to adjacent neurons in the AON (21). Cousens found that the DTT and AON showed similar responses but higher quantities of odor-selective neurons in the DTT, providing evidence that the tenia tecta contributes to olfactory processing. Bolding & Franks (2018) investigated the identification of odors in the OB mitral cells and the PC (32). They found that the OB cells drove responses to the PC. Iurilli & Datta (2017) investigated the spatial neurons in the PC versus the hardwired inputs in the plCoA (10). Iurilli and Datta found that both the plCoA and PC are involved in odor learning and innate behaviors driven by odors. Data was found via Github and CRCNS (Collaborative Research in Computational

Neuroscience), both provided by the authors. Data was aggregated to a single spreadsheet using MATLAB to open all the files and combine their respective fields.

Plotting

We used raster plots and peristimulus time histograms (PSTHs) for each cell-odor in the dataset to examine changes in neuronal firing rates. In the raster plots, each dot represents a neuronal spike, and each row represents one trial. PSTHs show the average firing rate (Hz) as a function of time (s), aligned to odor onset (red line)

To classify cells as excitatory, inhibitory, or non-responsive, we compared the firing rate after odor onset to the baseline (basal) firing rate using a Wilcoxon signed-rank test via MATLAB ($p = 0.01$). Neurons were labeled as excitatory if the firing rate rose above baseline and inhibitory if the firing rate fell below baseline for any time on the PSTH. Statistical significance of differences in proportions between regions and odor types was tested using two-tailed two-proportion z-tests via Jupyter Notebook.

To find cells with inhibitory/excitatory reactions, we generated cross-correlograms for neuron pairs. Cross-correlograms plot the spike count of a neuron pair as a function of time lag, revealing shared suppression or firing. Peaks close to zero lag indicate excitation, while troughs indicate inhibition.

To study rhythmicities in the brain, we ran autocorrelograms and took the fast Fourier transform (FFT) to determine the power of the theta, beta, and gamma frequencies. The median of the area under the curve (AUC) was compared with a two-tailed T-test with a significance level of 0.05.

Experimental Methods

Subjects

The mice used in this study were adult C57BL/6 mice bred at Drew University, aged 8 to 20 weeks. Mice were housed in same-sex plastic cages in a temperature and humidity-controlled enclosure with access to food and water as desired. Experiments were conducted in accordance with the National Institute of Health Guide for the Care and Use of Laboratory Animals (NIH Publications NO. 80-23) under monitoring by the Drew University Institutional Animal Care and Use Committee.

Surgery

During the surgery, subjects were anesthetized with urethane (target dose 1.5 mg/kg, intraperitoneal) and further supplemented with atropine (25 mg/kg). The additional atropine helped to reduce the respiratory secretion of the subjects further. Anesthetics were mounted in a standard stereotaxic frame. The level of anesthesia during the surgery was monitored by recording the respiration rate and hindlimb withdrawal. In the case that additional anesthesia was required, isoflurane was administered as needed. After being anesthetized, the skull of the subject was exposed, and a PFA-coated stainless-steel reference wire was placed in the right parietal lobe through a small craniotomy. Additionally, a stainless-steel head plate was affixed to

the skull with dental acrylic. Finally, a craniotomy was performed through the aperture, centered at the midline and 2.25 mm anterior to bregma.

Electrophysiological Recording

Mice were positioned on a headplate clamp on an anti-vibration platform. Values of electrical impulses were recorded in a closed Faraday cage within a laboratory fume hood to minimize electrical noise and external odors. A tungsten microelectrode (12MOhm, A-M Systems, Sequim, WA) was placed using a Huxley-style micromanipulator (MX310, Siskiyou, Grants Pass, OR). Recordings commenced from the moment at which spike waveforms were maintained stably for at least 5 minutes at depths >2.5 mm. When two or more recording sites occurred in the same electrode pass, the electrode was advanced until there was an absence of spikes from the initial recording, which was confirmed by inspection of oscilloscope traces. Neural signals were amplified and filtered using differential recordings (10,000X, 500 Hz - 3 kHz; A-M Systems Models 1800 or 3600) and digitized (20 kHz; POWER 1401, Cambridge Electronic Design, Cambridge, UK). Respiration was monitored throughout the session using a piezoelectric sensor positioned under the chest.

Stimulus Presentation

The electrophysiological recordings of action potentials and firing of neurons in the olfactory cortical areas in the mouse brain were done in two separate recording sessions. During the first session, the subject was presented with 14 individual odors composed of 7 ethyl esters, 6 terpenes, and mineral oil. On the second recording session, we presented a total of ten mixtures of esters and terpenes to the mouse to determine how mixing odorants impacts inhibition in the AON. We used three terpenes: Eucalyptol (T1), Linalool (T2), and Rose Oxide (T3), and three ethyl esters: Decanoate (E1), Octanoate (E2), and Valerate (E3).

After stable baseline recording, rates were measured for at least 5 minutes. Mineral oil was exposed as a control, followed by monomolecular odorants (Linalool, Citronellol, Geraniol, Alpha-Terpeniol, Ethyl Decanoate, Ethyl Octanoate, Rose Oxide, Ethyl Hexanoate, Eucalyptol, Ethyl Valerate, Ethyl Acetate, Ethyl Butyrate, Ethyl Propionate, Rotundone) in a pseudo-random order. Binary odorants were then presented in a structured sequence, comprised of three categories: terpene mixtures (Eucalyptol + Linalool, Eucalyptol + Rose Oxide, and Linalool + Rose Oxide), ethyl-ester mixtures (Decanoate + Octanoate, Decanoate + Valerate, and Octanoate + Valerate) and terpene–ester combinations (Eucalyptol + Decanoate, Linalool + Octanoate, Decanoate + Alpha-Terpineol, Octanoate + Rose Oxide).

Each odor in both recording sessions was presented for two seconds with a 28-second interstimulus interval (15 for mixture trials). Per mixture, 10 trials were done using a custom-built flow-dilution olfactometer controlled by Spike2 software (Cambridge Electronic Design). Odorants were diluted to reach 100 ppm in the vial headspace and delivered with oxygen gas as a medium through Teflon tubing at 1.0 L/min. One additional channel was reserved for mineral oil alone as a control stimulus. In order to minimize possible effects of odor source position on neuronal firing, odor tubes were fed through a manifold with a single outlet

port oriented rostrocaudally and positioned two cm from the nares. The manifold was cleaned daily to minimize contamination.

Identifying Recording Sites

The tungsten electrode was positioned to take recordings from the AON at 2.5 mm anterior and 1.0 mm lateral to bregma, and 2.0 mm ventral to the skull surface. Following the recording session, the brain was extracted and fixed in a formalin solution prior to histological processing to characterize the location of recording electrodes through light microscopy.

RESULTS

Firing Rate Changes

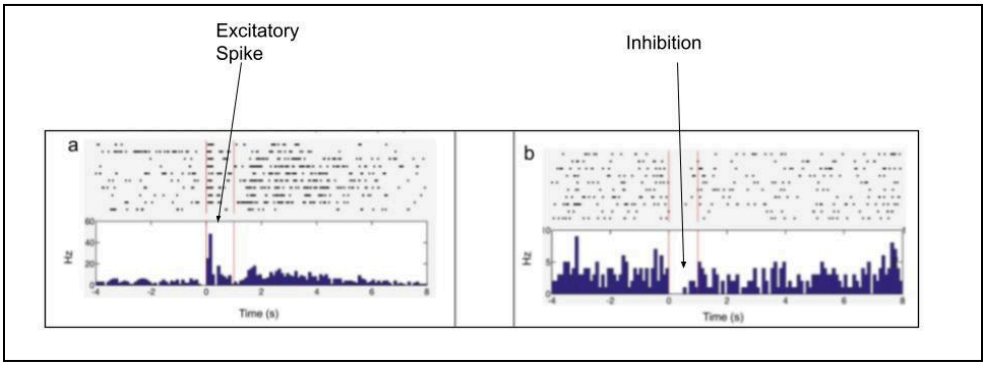

Figure 2. Excitatory and Inhibitory Piriform Cortex Neuronal Cells Exposed to Ethyl Butyrate. (Top) Raster plot. (Bottom) PSTH.

In the olfactory system, inhibition and excitation occur as odorants bind to ORNs. Our analysis indicates that olfactory neurons are primarily excitatory by generating action potential signals that are transmitted to the OB. The initial excitation of neurons, however, is regulated by inhibitory factors in multiple brain regions. We classified neurons as excitatory or inhibitory based on fluctuations in firing rates responding to odor onset. The raster plot in Figure 2(a) of an excitatory response illustrates an increase in spikes and action potentials following the presentation of odorants. Conversely, Figure 2(b) presents an inhibitory neuron, shown by the decrease in action potentials and neuron spikes after odor onset.

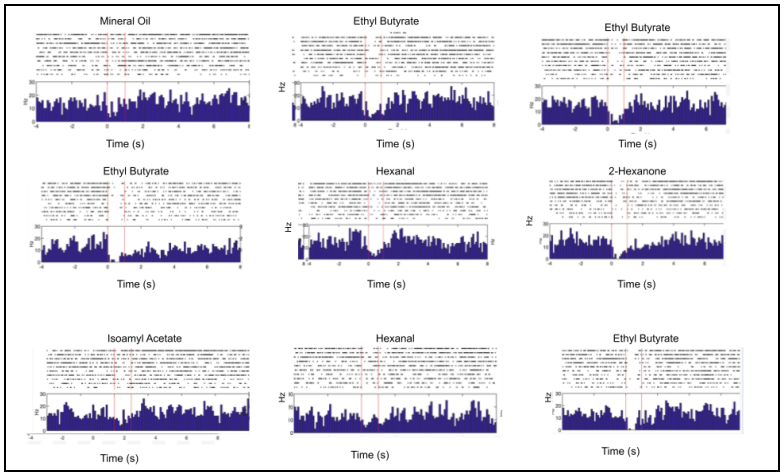

Figure 3. Broad Tuning: Raster Plots and PSTHs for a Neuron from the Piriform Cortex.

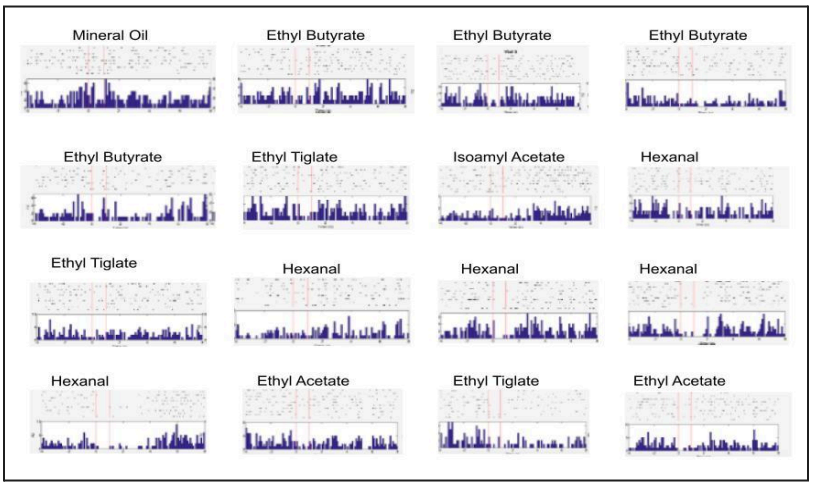

Figure 4. Narrow Tuning: Raster Plots and PSTHs for a Neuron from the Piriform Cortex.

Neurons in the olfactory system can also be classified by their tuning breadth. Broadly tuned neurons from the PC respond in an inhibitory manner to all presented odorants regardless of chemical structure (Figure 3). In contrast, narrowly tuned neurons only respond in an inhibitory manner to one odor (in this case, Hexanal) (Figure 4). This can be seen as most cell spikes are much lower, showing they are less responsive to odors.

Table I. Percentages of Inhibited, Excited, Non-Responsive Odor-Cell Pairs.

Region	Excitatory Odor-Cell Responses	Inhibitory Odor-Cell Responses	Non-Responsive Odor-Cell Responses
OB	157 (12.57%)	125 (10.01%)	967 (77.42%)
PC	100 (8.62%)	90 (7.76%)	970 (83.62%)
plCoA	8 (1.98%)	0 (0.00%)	397 (98.02%)

A summary of changes in firing rate across the olfactory cortex, shown in Table I, indicates that the OB exhibited the largest proportion of both inhibitory (10.01%) and excitatory (12.57%) responses compared to the other regions.

An analysis of Table I indicates that the OB and PC exhibited significantly higher proportions of inhibitory responses compared to the plCoA and TT (p-value < 0.05 according to a two-tailed 2-proportion z-test via Jupyter Notebook). However, the proportion of inhibitory responses did not significantly vary between the OB and PC (p-value > 0.05). The OB also demonstrated a significantly higher proportion of excitatory responses compared to all other regions. Although the PC illustrated a higher proportion of excitatory responses compared to the plCoA, this difference was not statistically significant when compared to the TT.

Table II. Percentages of Inhibited, Excited, Total Odor-Cell Pairs for Aldehydes and Esters.

Region	Odor Type	Excitatory Odor-Cell Responses	Inhibitory Odor-Cell Responses	Total Odor-Cell Responses
OB	Aldehyde	23 (39.7%)	35 (60.3%)	58
	Ester	34 (47.9%)	37 (52.1%)	71
PC	Aldehyde	27 (58.7%)	19 (41.3%)	46
	Ester	26 (44.1%)	33 (55.9%)	59
DTT	Aldehyde	4 (100%)	0 (0%)	4
	Ester	4 (100%)	0 (0%)	4
AON	Ester	2 (100%)	0 (0%)	2
plCoA	Aldehyde	1 (100%)	0 (0%)	1

An analysis of all inhibitory and excitatory cell responses to esters and aldehydes, summarized in Table II, revealed distinct responses between functional groups. In the OB, aldehydes evoked a majority inhibitory response (60.3%), while esters showed an almost even excitation/inhibition split (47.9% vs. 52.1%). However, the PC displayed a reversal with a majority excitatory response for aldehydes (58.7%) and a slightly inhibitory response to esters (55.9%). The smaller DTT, AON, and plCoA regions exhibited only excitatory responses, but their limited sample sizes prevent us from concluding. The OB exhibited significantly higher proportions of aldehyde and ester responses compared to the DTT, and the PC exhibited significantly higher ester responses than the DTT (p-value < 0.05 according to a two-tailed 2-proportion z-test). The proportion of responses between functional groups, however, did not significantly vary between other regions (p-value > 0.05).

Relation Between Neurons

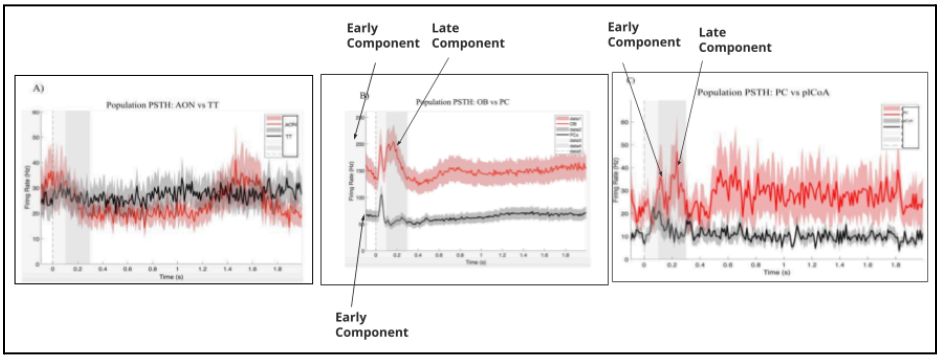

Figure 5. Population PSTH of Olfactory Regions. Figure A shows data from the Cousens study, B from Bolding & Franks, and C from Iurilli & Datta (21, 32, 10).

Relationships between neuron responses can appear in different brain regions. As shown in the Population PSTH generated in Figure 5, the AON and TT have a sinusoidal relationship. When the AON has an increased firing rate, the TT has a decreased firing rate, and vice versa. In contrast, Figure 5b showed a brief spike followed by a sustained increase in firing rate in the OB and a slow increase in population spiking that was rapidly suppressed in the PC. Figure 5b replicates Figure 2f of Bolding & Franks' study, validating our data. Figure 5c shows that the PC has higher firing rates than the plCoA (32).

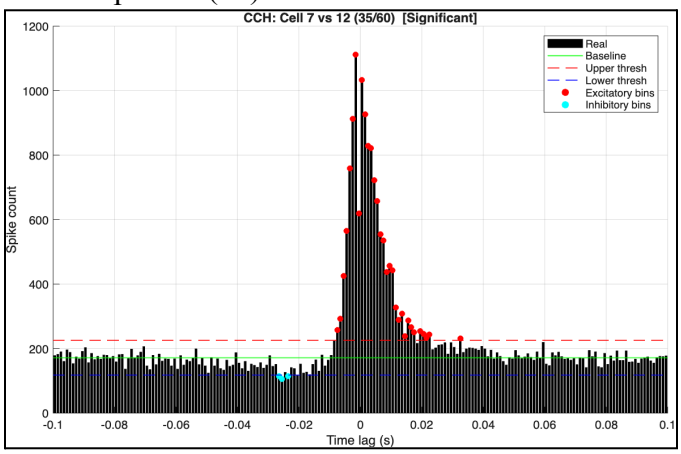

Figure 6. Cross-Correlogram of Cells in the Piriform Cortex. Red dashed: upper threshold; blue dashed: lower threshold; green line: null hypothesis (baseline spike count).

Neurons in the olfactory system can also share an inhibitory/excitatory reaction. Figure 6 shows a Cross-Correlogram between Cell 7 and 12 in the PC. This graph reveals a significant relationship in their firing patterns. The sharp cluster of black bars near zero, marked with red dots, indicates that Cell 7 consistently fires just before Cell 12—a hallmark of excitation. This excitation is statistically significant, as the spike count in these bins exceeds the upper threshold derived from shuffled trial data. Interestingly, we also observe one inhibitory bin around –25 ms, where the spike count drops below the expected lower threshold. This suggests that when Cell 12 fires roughly 25 ms before Cell 7, Cell 7 is less likely to spike. This could be a possible

inhibitory or suppressive interaction. Altogether, the data support a tightly-timed excitatory connection, possibly modulated by brief suppression.

Rhythmicity

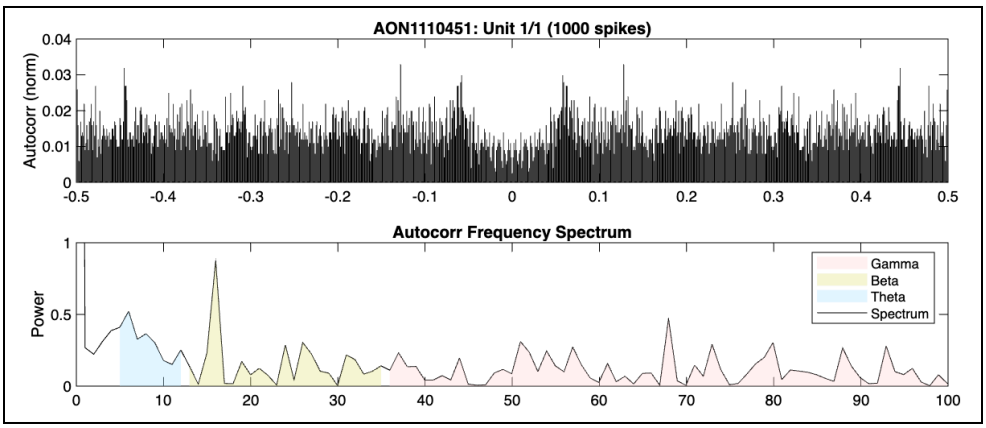

Figure 7. Rhythmicity of an AON neuron. (Top) Autocorrelogram, bar: likelihood of neuron firing after spike. (Bottom) FFT Frequency Spectrum, black line: power spectrum.

Rhythmicity, the cyclical changes in the sensitivity and function of the olfactory system, is explored by assessing the oscillatory properties of spike trains. As shown in Figure 7 (Top Panel) there are periodic peaks, indicating sustained oscillatory activity with a minimal bursting behavior. In Figure 7 (Bottom Panel), the frequency spectrum shows strong peaks at theta (5.99 Hz), beta (15.98 Hz), and gamma (67.93 Hz).

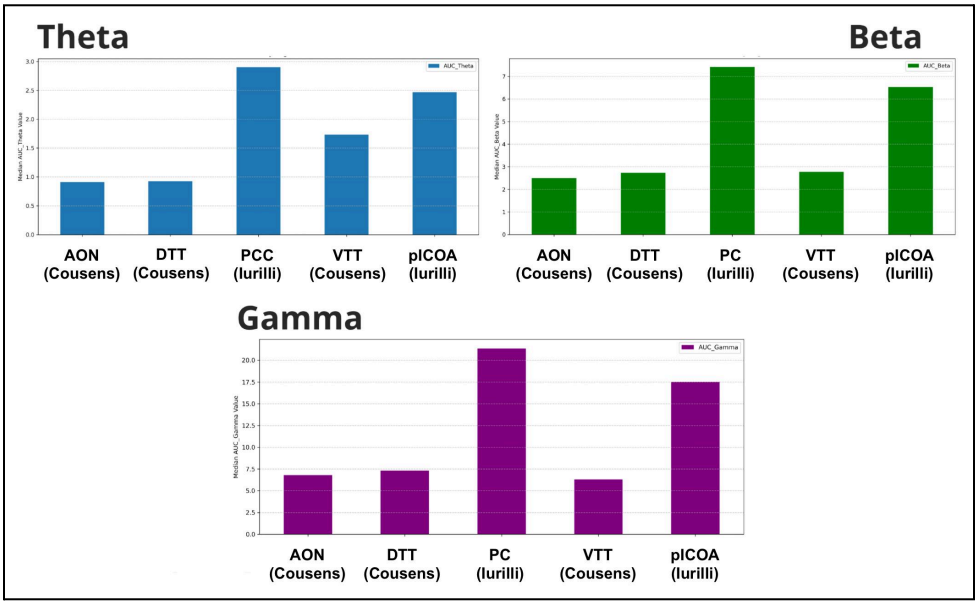

Figure 8. Median of the AUC of the FFT for Theta, Beta, and Gamma frequencies.

The extent of rhythmic patterns was also decreased in anesthetized versus awake mice: there was a significant difference in all brain region pairings between the mice presented in the Cousens study (used anesthesia) and the Iurilli study (did not use anesthesia) except for the VTT

and the PC or plCOA in the theta and beta frequencies (p-value < 0.05 for a two-tailed T-test) (Figure 8) (21,10). This could present a discrepancy in our data analysis between the anesthetised versus awake mice.

Responses to Mixtures

In our own experiment, we examined how odorant mixtures affect neurons in the AON. We predicted that the degree of mixture suppression would relate to the degree of similarity between odorants, with similar classes of odorants (ex., terpene-terpene or ester-ester) resulting in the most suppression, and less suppression across classes (e.g., terpene-ester). When multiple odorants activate overlapping ORNs, the glomeruli can mutually suppress each other and cause inhibition.

All mixtures returned non-responsive after odor onset (Figure 9). This is due to the small sample size of our experiment.

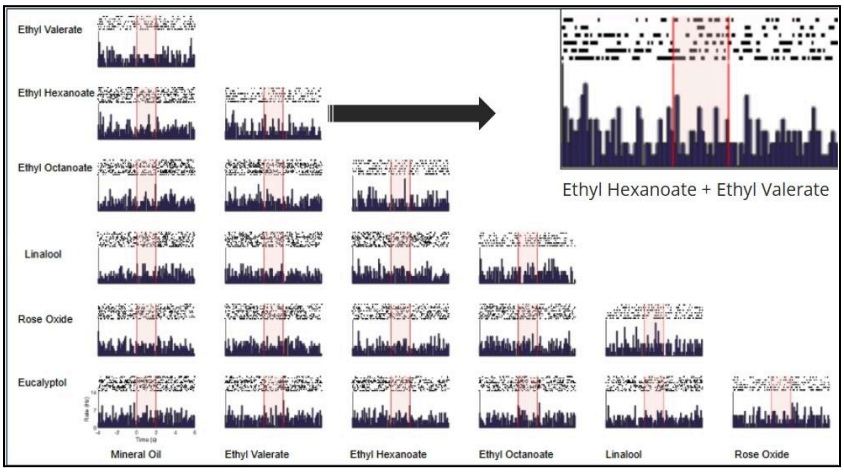

Figure 9. Histograms of Neurons in the AON for Odor Mixtures. Shows spike firing rate (Hz) v. time (s).

DISCUSSION

Using meta-analysis and experimental procedures, we examined how information and odor processing vary throughout the olfactory system by analyzing patterns of inhibition. Combining data collected from various electrophysiological studies and analyzing patterns of odor-evoked spike activity, we found various patterns between the location and function of a cortical region and its usage of inhibition. Neural activity observed from higher order cortical regions, such as the OB and PC, exhibited high inhibitory and excitatory responses. In contrast, the plCoA and TT were less responsive, likely due to their role in higher-order processing.

We first sought to characterize the extent to which neurons within these olfactory systems exhibited inhibitory responses to monomolecular odorants, and our findings show that inhibition is most prevalent in the OB, with the PC also showing substantial amounts of inhibition. This observation suggests that the olfactory system is organized into a hierarchy that can be classified by distinct patterns of neural responsiveness across various cortical regions. Among all the observed regions, these early-stage structures exhibited the highest level of odor-invoked activity, with the OB exhibiting the greatest amount of inhibitory (10.01%) and

excitatory (12.57%) responses (Figure 2). Such patterns in our data, and indicated in Figures 3 and 4, suggest that the OB uses broad tuning to selectively amplify neural signals specific to certain odors while simultaneously suppressing overlapping signals. This allows it to initiate responses that are specific to the presented odorant. As the signal recognized in the OB progressed into the PC, there was no significant difference in neuron responses. In this region, the tuning is similar, considering it has moderately high levels of both inhibitory (8.62%) and excitatory (7.76%) responses. Exemplifying the PC's role in connecting early processing and high-order interpretation of stimuli, this pattern across studies supports how the PC uses population coding to distinguish between a vast number of odors. Unlike the OB and PC, the high-order cortical areas, such as the plCoA and the TT, exhibited a notable decrease in response rates with low levels of excitation (6.1-1.98%) and little to no recordings of inhibition (0-0.2%). This suggests that these regions of the olfactory system do not rely on the suppression and/or amplification of stimuli through inhibition but rather focus on interpretation linked to higher-order integration of odor information and associative memory (24).

The framework of this hierarchical pathway is strongly linked to inhibition patterns that shape how information is encoded and transmitted throughout the olfactory system. Strong inhibition observed in the OB and PC suggests that these regions use the suppression of excitability to regulate the initial representation of odors (Table 1). Feedforward inhibition could be particularly significant in the OB when enhancing the precision of tuning curves among mitral and tufted cells to ensure they are selectively responding to odorants. This finding aligns with existing literature that suggests feedforward inhibition from the ORNs activates granule cells, which suppress mitral and tufted cell activity (25). In the PC, inhibition appears to be used to enhance the accuracy of odor perception by suppressing unnecessary signals and thus filtering and refining information from the OB, which is consistent with findings from Franks et al. (2011), who showed that recurrent inhibition stabilizes odor representations and sharpens the timing and specificity of cell firing. The relative absence of inhibition in the plCoA and TT reinforces the claim that these regions are responsible for associative processing, in contrast to the primary cortical areas that rely on inhibition for stimulus encoding and recognition. Instead, these regions likely rely on modulatory or contextual signals rather than sensory-based firing to integrate odor-invoked responses. Our findings indicate that inhibition circuits vary across olfactory regions depending on their functional demands rather than simply being scaled down along the olfactory pathway (26).

When analyzing data of ester and aldehyde functional groups, we found that in the PC, both odor types induced similar excitatory (~40%) and inhibitory (~60%) responses. In contrast, the DTT only produced excitation (~100%) when exposed to the functional groups. There was no significant difference in responses between functional groups (Table 2). This suggests that while the PC experiences excitation and feedforward inhibition, the DTT experiences mostly excitatory neurons when exposed to aldehydes and esters. The similar responses between functional groups reflect overlapping receptor activation. The OB has noticeable differences in inhibition and excitatory patterns based on functional groups; aldehydes evoke mainly inhibitory responses, while esters evoke approximately similar proportions of excitatory and inhibitory responses. Surprisingly, neurons observed in the PC majorly showed excitatory responses for aldehydes and slightly lower proportions of inhibitory responses. These responses further justify the functional roles of the OB and PC and their suppression tendencies. High-order regions such

as the DTT, AON, and plCoA had exclusively excitatory responses, although we were only able to analyze a minimal number of neurons in this area, which could possibly skew our results.

When comparing cell pairs across regions, our population PSTHs indicate that neural firing patterns vary based on the functional order of the neuron (Figure 6). Activities in the AON and the DTT reveal a potential sinusoidal relationship where one of the cells in the pair remains excited and the other is not. This finding suggests that neurons in these regions potentially play complementary roles in the olfactory system that require the balancing of responses to enhance broader feedback systems. The particularly notable spike in the AON following the second mark, about 1.3-1.6 seconds after odor onset, reflects how higher-order cortical regions typically have delayed processing compared to regions such as the OB (Figure 5a). Consistent with the aforementioned processing hierarchy, the OB and PC showed large and rapid spikes in firing rates immediately after odor onset. The PC, however, maintained consistent levels of elevated activity which affirms that it plays a greater role in encoding sensory information (Figure 5b). This responsiveness corresponds with the denser number of axonal projections the PC receives from the LOT. Regions such as the plCoA and the DTT illustrated comparatively lower proportions of firing rates, indicating sparse coding which is known to assist in connecting sensory input to emotional or behavioral response.

We also observed different oscillatory rhythms by implementing a FFT in our autocorrelogram. The power of theta, beta, and gamma frequencies was significantly decreased in anesthetized mice when comparing the data from Cousens (2020) and Iurilli & Datta (2017). This presents a potential source of error in our other data analysis comparing the two (21, 10).

Finally, we designed and began a novel experiment testing how mixtures affect inhibitory responses in the AON. We expect that mixtures composed of chemically similar odorants will elicit greater response suppression due to overlapping receptor activation and local circuit interactions, while diverse mixtures may produce a greater variety of effects. Unfortunately, no neurons responded to any of the odorants (Figure 9). We suspect this is due to the small sample size recorded. These results are supported by previous findings on mixture suppression and offer insight into how inhibition influences the neural representation of odor. Despite having limited data from our experiment, this study provides insight into the effects of mixture suppression in AON, which has been minimally researched in previous studies. Future studies can use our preliminary research and results as a stepping stone for more rigorous future research that expands our knowledge on the AON.

Limitations

Although our experimentation and Cousens (2020) used mice anesthetized with urethane, the data we compared with those in Bolding & Franks (2018) and Iurilli & Datta (2017) used mice without an anesthetic (21, 32, 10). The electrophysiological recordings we analyzed used slightly different procedures. Mice without an anesthetic have the ability to sniff, possibly resulting in those two studies having increased levels of neuron activity.

While the studies by Cousens and Iurilli & Datta both used adult male C57BL/6 mice, Bolding and Franks used adult offspring of *Emxl-cre* (21, 10, 32). In addition, even though the

studies by Cousens and Iurilli & Datta used the same breed of mice, differences are evident (21, 10). These include differences in mouse ages—the mice were 8 to 20 weeks old in Cousens' experiment and 5 to 7 weeks old in the study by Iurilli & Datta—in addition to possible weight variations. Therefore, their olfactory systems may function differently, and the conclusions we drew by comparing the different articles may be slightly skewed. Additionally, the different parts of the surgery procedure could produce statistical variability, such as placing the electrode in the brain or placing the Q-fixation plate. Because of the slight inconsistencies aforementioned in the data analyzed, different studies in our meta-analysis may produce slight modulations in the results.

Future Analysis

Investigating how chemically diverse functional groups are molecularly represented in the brain allows us to learn how different odors are perceived and stored. Studies can also analyze non-traditional brain regions like the LEC and the Medial Entorhinal Cortex (MEC) (27). These brain regions are essential in supporting odor-context association and long-term memory, but they remain understudied in many olfactory studies. Lastly, several studies, such as one by O'Sullivan et al. (2020), display the importance of inhibition in the auditory system. Since our research provided intriguing findings on inhibition's importance in the olfactory system, logical future analysis could involve studying inhibition in additional systems (28). Studying functional groups outside of esters, terpenes, and aldehydes would also further the current understanding of the olfactory system. Since humans can detect many functional groups like thiols (-SH), oximes (-NOH), and nitro groups (-NO2) more easily than a single elemental compound, it is important to study all functional groups and their interactions (29).

Applications

In addition to gaining a foundational understanding of inhibitory action in the brain, this work can be applied in the fields of neurodegenerative conditions and viral treatments. In neurodegenerative diseases, olfactory deficits appear early and can tend to precede changes in motor and cognitive abilities (30, 13). The findings from this study can inform future efforts to develop olfactory-based diagnostic tools or early intervention strategies. In viral diseases like COVID-19, the olfactory system can be damaged by support cells of alternating neural signaling. Recent research, however, suggests that viral diseases such as SARS-CoV-2 may also affect central cortical areas, including the olfactory bulb and downstream cortical regions (31). Deficits in inhibition may contribute to the persistence of viral symptoms such as the loss of smell. Since this study explores patterns of inhibition across the olfactory system, our findings may guide therapeutic interventions aimed at restoring olfactory abilities due to viral infections or neurodegenerative disorders.

ACKNOWLEDGEMENTS

We would like to thank and acknowledge the Office of the Secretary of Higher Education of New Jersey, the Overdeck Family Foundation, Novartis, Bristol Myers Squibb, and GSNJS Alumni & Parents of Alumni for their gracious donations. We would also like to extend our gratitude to Dr. Graham Cousens for his guidance, expertise, and prior work in this field. In

addition, we would also like to recognize Harris Naqvi for his assistance in this project. Finally, we would like to thank Dr. Adam Cassano, Dr. Stephen Dunaway, the counselors of the GSNJS, and Drew University for this opportunity.

REFERENCES

1. Purves, D. (1970, January 1). *The olfactory epithelium and olfactory receptor neurons*. Neuroscience. 2nd edition. https://www.ncbi.nlm.nih.gov/books/NBK10896/
2. Genovese, F., Reisert, J., & Kefalov, V. J. (2025, July 21). *Sensory transduction in photoreceptors and olfactory sensory neurons: Common features and distinct characteristics*. Frontiers. https://www.frontiersin.org/journals/cellular-neuroscience/articles/10.3389/fncel.2021.761416/full
3. Tufo, C., Poopalasundaram, S., Dorrego-Rivas, A., Ford, M. C., Graham, A., & Grubb, M. S. (2022, February 1). *Development of the mammalian main olfactory bulb*.
4. M;, M. K. Y. K. (n.d.). *Maps of odorant molecular features in the mammalian olfactory bulb*. Physiological reviews. https://pubmed.ncbi.nlm.nih.gov/16601265/
5. Branigan, B. (2023, May 1). *Physiology, Olfactory*. StatPearls [Internet]. https://www.ncbi.nlm.nih.gov/books/NBK542239/
6. K;, N. S. Y. Y. (n.d.). *Mitral and tufted cells differ in the decoding manner of odor maps in the rat olfactory bulb*. Journal of neurophysiology. https://pubmed.ncbi.nlm.nih.gov/14960563/
7. Bohbot, J. D., & Pitts, R. J. (2025, July 20). *The narrowing olfactory landscape of insect odorant receptors*. Frontiers. https://www.frontiersin.org/journals/ecology-and-evolution/articles/10.3389/fevo.2015.00039/full
8. Charlier, L., Topin, J., Ronin, C., Kim, S.-K., Goddard, W. A., Efremov, R., & Golebiowski, J. (2012, December). *How broadly tuned olfactory receptors equally recognize their agonists. human OR1G1 as a test case*. Cellular and molecular life sciences : CMLS. https://pmc.ncbi.nlm.nih.gov/articles/PMC11115053/#:~:text=We%20perceive%20odors%20through%20a,encountered%20in%20more%20specific%20systems.
9. Reisert, J., & Restrepo, D. (2009, September). *Molecular tuning of odorant receptors and its implication for odor signal processing*. Chemical senses. https://pmc.ncbi.nlm.nih.gov/articles/PMC2733323/
10. Iurilli, G., & Datta, S. R. (2017, March 8). *Population coding in an innately relevant olfactory area*. Neuron. https://pmc.ncbi.nlm.nih.gov/articles/PMC5370575/
11. Fournier, J., Müller, C. M., & Laurent, G. (2015, April). *Looking for the roots of cortical sensory computation in three-layered cortices*. Current opinion in neurobiology. https://pmc.ncbi.nlm.nih.gov/articles/PMC4898590/
12. Bao, X., Raguet, L. L., Cole, S. M., Howard, J. D., & Gottfried, J. (2016, April 28). *The role of piriform associative connections in odor categorization*. eLife. https://pmc.ncbi.nlm.nih.gov/articles/PMC4884078/
13. RL;, D. (n.d.). *Olfactory dysfunction in parkinson disease*. Nature reviews. Neurology. https://pubmed.ncbi.nlm.nih.gov/22584158/
14. Wilson, Donald A., & Sullivan, Regina M. (2011). Cortical Processing of Odor Objects. Neuron, 72(4), 506–519. https://doi.org/10.1016/j.neuron.2011.10.027

15. Kay, R. B., & Brunjes, P. C. (2014). Diversity among principal and GABAergic neurons of the anterior olfactory nucleus. Frontiers in Cellular Neuroscience, 8. https://doi.org/10.3389/fncel.2014.00111
16. GA;, C. (2020, July 22). *Characterization of odor-evoked neural activity in the olfactory peduncle*. IBRO reports. https://pubmed.ncbi.nlm.nih.gov/32793841/
17. Xu, W., & Wilson, D. A. (2012). Odor-evoked activity in the mouse lateral entorhinal cortex. Neuroscience, 223, 12–20. https://doi.org/10.1016/j.neuroscience.2012.07.067
18. Kee T;Sanda P;Gupta N;Stopfer M;Bazhenov M; (n.d.). *Feed-forward versus feedback inhibition in a basic olfactory circuit*. PLoS computational biology. https://pubmed.ncbi.nlm.nih.gov/26458212/
19. Roux, L., & Buzsáki, G. (2015). Tasks for inhibitory interneurons in intact brain circuits. Neuropharmacology, 0, 10–23. https://doi.org/10.1016/j.neuropharm.2014.09.011
20. Kay LM;Beshel J;Brea J;Martin C;Rojas-Líbano D;Kopell N; (2009, April). *Olfactory oscillations: The what, how and what for*. Trends in neurosciences. https://pubmed.ncbi.nlm.nih.gov/19243843/
21. Cousens, G. A., & Muir, G. M. (2006). *Using extracellular single-unit electrophysiological data as a substrate for investigative laboratory exercises*. Journal of undergraduate neuroscience education : JUNE : a publication of FUN, Faculty for Undergraduate Neuroscience. https://pmc.ncbi.nlm.nih.gov/articles/PMC3592630/
22. Kubska, Z. R., & Kamiński, J. (2021, March 30). *How human single-neuron recordings can help us understand cognition: Insights from memory studies*. Brain sciences. https://pmc.ncbi.nlm.nih.gov/articles/PMC8067009/
23. Stettler, D. D., & Axel, R. (2009). Representations of Odor in the Piriform Cortex. Neuron, 63(6), 854–864. https://doi.org/10.1016/j.neuron.2009.09.005
24. Otazu, G. H., Chae, H., Davis, M. B., & Albeanu, D. F. (2015, June 17). *Cortical feedback decorrelates olfactory bulb output in awake mice*. Neuron. https://www.sciencedirect.com/science/article/pii/S0896627315004304
25. Burton, S. D., & Urban, N. N. (2015, October 21). *Rapid feedforward inhibition and asynchronous excitation regulate granule cell activity in the mammalian main olfactory bulb*. The Journal of neuroscience : the official journal of the Society for Neuroscience. https://pmc.ncbi.nlm.nih.gov/articles/PMC4683680/#sec19
26. Geramita, M. A., Burton, S. D., & Urban, N. N. (2016, June 28). *Distinct lateral inhibitory circuits drive parallel processing of sensory information in the mammalian olfactory bulb*. eLife. https://pmc.ncbi.nlm.nih.gov/articles/PMC4972542/
27. M;, B. G. C. (n.d.). *Olfactory inputs activate the medial entorhinal cortex via the hippocampus*. Journal of neurophysiology. https://pubmed.ncbi.nlm.nih.gov/10758103/
28. M;, O. C. A. (n.d.). *Disruption of early or late epochs of auditory cortical activity impairs speech discrimination in mice*. Frontiers in neuroscience. https://pubmed.ncbi.nlm.nih.gov/31998064/
29. Genva, M., Kenne Kemene, T., Deleu, M., Lins, L., & Fauconnier, M.-L. (2019, June 20). *Is it possible to predict the odor of a molecule on the basis of its structure?*. MDPI. https://www.mdpi.com/1422-0067/20/12/3018
30. KA;, A. J. L. (n.d.). *Olfactory bulb involvement in neurodegenerative diseases*. Acta neuropathologica.
31. de Melo GD;Lazarini F;Levallois S;Hautefort C;Michel V;Larrous F;Verillaud B;Aparicio C;Wagner S;Gheusi G;Kergoat L;Kornobis E;Donati F;Cokelaer

T;Hervochon R;Madec Y;Roze E;Salmon D;Bourhy H;Lecuit M;Lledo PM; (2021, June 2). *Covid-19-related anosmia is associated with viral persistence and inflammation in human olfactory epithelium and brain infection in hamsters*. Science translational medicine. https://pubmed.ncbi.nlm.nih.gov/33941622/

32. Bolding, K. A., & Franks, K. M. (2018). Recurrent cortical circuits implement concentration-invariant odor coding. *Science*, *361*(6407). https://doi.org/10.1126/science.aat6904

APPENDIX A

Anterior olfactory nucleus (AON)
Dorsal tenia tecta (DTT)
Entorhinal cortex (EC)
Fast Fourier Transform (FFT)
Lateral Entorhinal cortex (LEC)
Lateral olfactory tract (LOT)
Olfactory sensory neuron (OSN)
Olfactory receptor neuron (ORN)
Olfactory tubercle (OT)
Piriform cortex (PC)
Posterolateral cortical amygdala (plCoA)
Tenia tecta (TT)
Ventral tenia tecta (VTT)

APPENDIX B

https://github.com/survani-sinha/NeuroOlfaction